IET Research Journals

Submission Template for IET Research Journal Papers

IET Journals
The Institution of Engineering and Technology

Protection Coordination Scheme for Distribution Networks with High Penetration of Photovoltaic Generators

ISSN 1751-8644
doi: 0000000000
www.ietdl.org

Bahador Fani[1,2], *Hadi Bisheh*[1,2], *Iman Sadeghkhani*[1,2*]

[1] *Smart Microgrid Research Center, Najafabad Branch, Islamic Azad University, Najafabad 85141-43131, Iran*
[2] *Department of Electrical Engineering, Najafabad Branch, Islamic Azad University, Najafabad 85141-43131, Iran*
* *E-mail: sadeghkhani@pel.iaun.ac.ir*

Abstract: The installation of photovoltaic (PV) systems is gaining great attention due to the matured PV technology and the lowered price of PV modules. With an increasing penetration of PV systems, the selectivity of distribution network protection may be affected which results in undesirable de-energization of loads, damage of network equipment, and reduction of reliability. This paper presents a method to preserve the protection coordination considering future PV systems installation with any penetration level and different locations along the distribution feeder. Depending on the accessibility of protection device settings or PV control parameters, the proposed method modifies the existing characteristic curve of overcurrent devices or limits the output current of PV sources, respectively. The proposed strategy does not change the structure of existing distribution network protection system and can be also implemented in the old and non-programmable relays. Meanwhile, it does not need the communication links. The merits of the proposed method are demonstrated through several case studies using the Isfahan distribution network.

1 Introduction

In recent years, the electronically coupled distributed generations (DGs) have been gaining popularity among industries and utilities due to easy installation and operation, possibility of using the renewable energies such as photovoltaic (PV) systems, and their high efficiency [1–5]. The PV systems are connected to the grid in a centralized or distributed manner depending on their capacity. The former architecture is usually used for the utility-scale PV power plants up to 100 MW capacity [6], while the latter architecture is employed for the low capacity PV systems such as building integrated ones. In addition to feeding the local loads, the distributed PV systems can deliver their extra power to the grid to increase the system reliability in the cases of voltage drop and lack of power generation [7, 8].

In the presence of PV sources, there are two protection issues: (1) protection of PV installations against the electric shock [9], overcurrent [10], and lightning and surge [11] and (2) considering the effect of PV systems on the network protection that is the focus of this paper. In the normal operation of the network, the presence of PV systems have numerous advantages for both utility and consumers. However, distributed installation of PV systems in the feeders changes the current profile of the distribution network [12]. It brings new challenges for conventional protection systems including overcurrent relays (OCRs) and their coordination may be no longer preserved properly [13]. The impact of PV systems on the distribution network during a fault condition is completely different with the normal operation which may disrupt the protection system operation. This disruption may increase the short-circuit level, change the current direction, and sympathetically trip the circuit breakers [14, 15]. It makes necessary to thoroughly re-examine the distribution network protection. In recent years, with an increasing penetration of PV systems, the interconnection protection requirements are reformulated with a view of adapting them to larger PV systems [16].

There are two main strategies to improve the performance of the protection system in the presence of PV sources. The first strategy disconnects the PVs during the fault to prevent change of network current profile [17, 18]. However, it reduces reliability and increases possibility of synchronization problems during reconnection of PVs [15]. Also, in this strategy, high speed fuses and fast characteristic curves for relays can not be used.

By modifying the protection system design, using the computational algorithms, or limiting the PV generation, the second category schemes aim to provide the proper operation of the protection devices [19–28]. The utilization of the new and programmable relays, directional relays, and distance relays are proposed in [19–23]. Moreover, [24] and [25] preserve the protection coordination by implementing the multi-agent systems and the communication links among protection devices, respectively. Since the data exchange is online, these methods are accurate, fast, and effective. However, the high cost and low reliability of such systems are their main disadvantages.

Optimal locations of DGs are identified using the computational algorithms in [26, 27] to solve the protection miscoordination problem. Also, [27] determines the optimal size of DGs to restore the protection system coordination. In addition to the complexity, these methods limit the possible DG locations. Also, the performance of these methods may be deteriorated when the network topology changes. To reduce the effect of DGs on the fault current, [28] limits the current of all PV sources of the network while [29, 30] use the fault current limiter (FCL). However, high cost, low reliability, and accurate sizing are the main disadvantages of using external devices.

The effects of changing the penetration level and location of PVs on the effectiveness of the protection systems are not adequately addressed yet. This paper presents a procedure to preserve the coordination of protection system for any penetration level and different locations of PV sources. Depending on the accessibility of protection system settings or PV control system parameters, the proposed scheme restores the protection coordination using two strategies. The first strategy modifies the characteristic curve of the protection device which is completely based on the existing standards and can be applied to all protection devices. Regarding to the penetration level and location, the second strategy determines those PV sources which further affect the protection system. By further limiting the output current of these PVs than that of other ones, the protection coordination is preserved during the fault condition. Thus, unlike [28], the second strategy does not reduce the output power of

those PVs which less affect the protection system. It is worth mentioning that the new settings are adjusted once. The proposed method does not require the communication link. Also, it does not change the protection system structure, even in the presence of the old and non-programmable relays.

This paper is organized as follows. Sections 2 investigates the impact of high penetration of PV sources on the distribution feeder protection system. Section 3 determines those conditions in which the protection coordination is lost and presents the solution to restore the protection coordination. Section 4 is dedicated to the proposed protection scheme. Simulation case studies are presented in Section 5 to verify the effectiveness of the proposed strategies. Finally, Section 6 gives the conclusions.

2 Investigation of PV Sources Impact on the Network Protection System

Variation of sun radiation during different hours of the day changes the penetration level of PV systems. The penetration level of PV systems in a feeder is defined as [31, 32]

$$\text{Penetration Level} = \frac{\sum_{m=1}^{n} P_{\text{PV}_m}}{\sum_{j=1}^{d} P_{\text{Load}_j}} \times 100, \qquad (1)$$

where P_{PV} and P_{Load} are the injected power of the PV source to the network and the network load, respectively. n and d are the number of PV sources and network loads, respectively. Since the relays of distribution feeders are usually adjusted using the relay current in the fault condition, a change in this current may disrupt or even improve the relay performance in some conditions.

In the distribution feeders, the current flows from the upstream network to the consumers located at the downstream feeder. Depending on the location and penetration level, the PV sources decrease the injected current of the upstream network. In the presence of PV systems, the fault current sources are both the upstream network and the PV sources. The magnitude of protection relay current depends on the location of PV sources along the feeder. The impedance between the upstream network and the fault location determines the fault current magnitude. By installing the PV systems along the feeder, the current through the relays of the downstream network may be greater than that of the upstream network. In this condition, the performance of the protection system is affected by the PV sources. Installing the PV systems at the downstream of the main relay do not disrupt the protection system operation. However, when the PV systems are installed between the downstream and upstream relays as the main and backup protections, respectively, the protection coordination may be lost. On the other hand, although the installation of PV systems at the upstream of the backup protection equally changes the current through the main and backup relays, it may disrupt the protection coordination in some conditions.

Fig. 1 shows a radial distribution network in which both the backup relay OCR1 and the main relay OCR2 are the conventional overcurrent relays. When no PV source is installed in the distribution network, the main and backup relays coordinately operate with a proper coordination time interval (CTI) for the short circuit current I_S, as shown in Fig. 2. To study the protection coordination, the minimum and maximum fault current through the main and backup relays $I_F^{\min}$ and $I_F^{\max}$ as the most critical cases are considered. Based on these currents, the operating times of the relays are determined to preserve the protection coordination. Indeed, in the conventional protection system, OCR1 and OCR2 correctly operate in the current range $\left[I_F^{\min}, I_F^{\max}\right]$ with proper CTI between their characteristic curves.

When the PV systems are installed between the main and backup relays and a fault occurs at the point F in Fig. 1, the current through OCR1 decreases while the current through OCR2 increases. With an increasing penetration of PV systems, their injected currents increase and consequently, the current through the backup relay OCR1 more

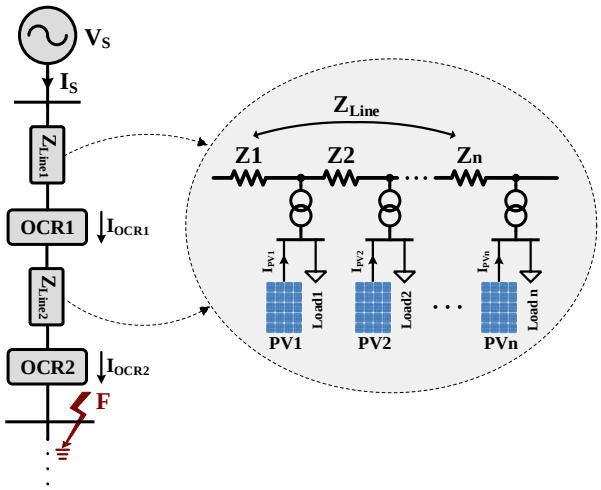

Fig. 1: Schematic diagram of a radial distribution feeder in the presence of PV systems.

decreases. If the decreased OCR1 current is between $I_F^{\min}$ and $I_F^{\max}$, PV connection improves the protection coordination by providing a safe interval for operating time of the backup relay. However, for a certain penetration level of PV systems, the current through OCR1 is smaller than the lower limit $I_F^{\min}$. In this condition, the operating time of OCR1 is greater than the thermal limit of the network conductors. During the fault condition, the high current through the conductors increases their temperature which may damage the network equipment. Based on the IEC 60909 [33], the thermal limit of the conductors is determined as

$$I^2 t \leq K^2 S^2, \qquad (2)$$

where I is the RMS value of the fault current in ampere, t is the fault duration in second, and S is the cross-sectional area of the conductor in square millimeters. K is a factor that depends on the conductor material. This standard states that the maximum fault clearing time should be lower than the thermal limit. To satisfy this condition, the characteristic curves of the protection system should be located below the thermal limit curve (I^2t curve), as shown in Fig. 2. When the current through the backup relay OCR1 is smaller than $I_F^{\min}$, the coordination of protection relays of Fig. 1 is lost; OCR1 does not

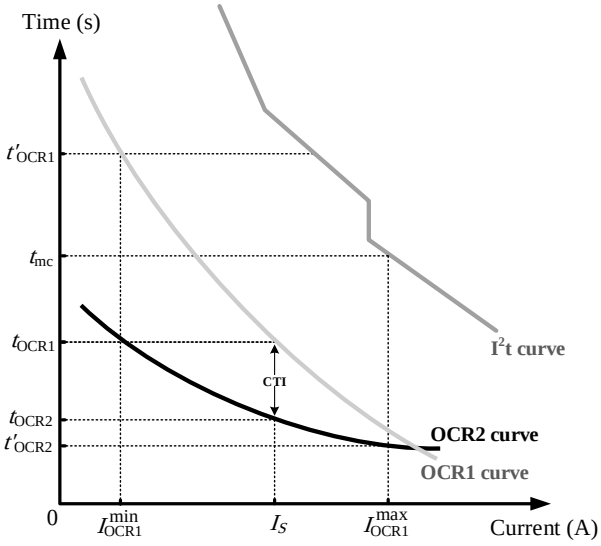

Fig. 2: Characteristic curves of the main and backup protection relays.

operate as the backup protection and it likely operates in its overload region.

If the PV systems are located upstream from both main and backup relays, the current through the OCR1 and OCR2 is greater than I_S during a fault. By increasing the penetration level of PV systems in the network, the current through the protection relays more increases and consequently, the operating times of the main and backup relays are reduced based on their protection characteristic curves. In a specified penetration level of PV sources, the protection coordination may be lost if the characteristic curves of these relays are adjusted in such a way that increasing the current higher than $I_F^{\max}$ decreases the time interval between them. In this condition, a proper strategy is required to restore the protection coordination. It should be noted that modification of protection coordination in a specified penetration level of PV systems may result in mal-operation of protection system for other penetration levels.

3 Protection Coordination in the Presence of PV Sources in the Network

Consider the system shown in Fig. 1 without its PV systems. When a fault occurs at the downstream of main protection (point F), the currents through the OCR1 and OCR2 are

$$I_{\mathrm{OCR1}} = I_{\mathrm{OCR2}} = I_S = \frac{V_S}{Z_T}, \tag{3}$$

where I_S is the injected fault current of the network, V_S is the network voltage, and Z_T is the total impedance between the upstream network and the fault location. Since the currents through the both relays are same, the backup relay operates with a proper time interval CTI if the main relay fails. When one PV source is located between two protection relays, the currents through the backup and main relays are different, and they are calculated using (4) and (5), respectively, as

$$I_{\mathrm{OCR1}} = I_S - \left(\frac{Z_1 + Z_F}{Z_T}\right) I_{\mathrm{PV1}}, \tag{4}$$

$$I_{\mathrm{OCR2}} = I_S + \left(1 - \frac{Z_1 + Z_F}{Z_T}\right) I_{\mathrm{PV1}}, \tag{5}$$

where I_{PV1} is the injected current of the PV source, Z_1 is the impedance between the PV source and the main relay, and Z_F is the fault resistance plus the impedance between OCR2 and fault location. Depending on the PV location and its distance to the fault, the output current of the PV source may increase the fault current. It reduces the injected current of the upstream network, because the distance of the network to the fault usually is greater than that of the PV source to the fault. Thus based on (4) and (5), depending on the PV location and capacity, I_{OCR1} decreases while I_{OCR2} increases.

3.1 Presence of PV Sources Between the Main and Backup Relays

In the case of PVs located between the main and backup protections and occurring a fault at the downstream of OCR2, the currents through the backup and main relays are expressed as

$$I_{\mathrm{OCR1}} = \frac{1}{Z_T}\left[V_S - \sum_{m=1}^{n} I_{\mathrm{PV}_m}\left(Z_F + \sum_{i=1}^{m} Z_i\right)\right], \tag{6}$$

$$I_{\mathrm{OCR2}} = \frac{1}{Z_T}\left[V_S + \sum_{m=1}^{n}\left(I_{\mathrm{PV}_m} Z_T - I_{\mathrm{PV}_m}(Z_F + \sum_{i=1}^{m} Z_i)\right)\right], \tag{7}$$

where I_{PV_m} is the current of mth PV located between two protection relays and Z_i is the impedance between two consecutive PVs. Equations (6) and (7) show that increasing the penetration level of PV sources results in reduction of current through the backup relay and increment of current through the main relay. Consequently, the backup protection operates with more time delay than the initial coordination interval; even its delay may be greater than the thermal limit curve of the network conductors.

Fig. 2 shows that for the fault current I_S, OCR2 operates at t_{OCR2}. If this relay fails, after the time interval CTI, OCR1 operates at t_{OCR1} before exceeding the thermal limit of the network conductors. If the penetration level of the PV sources between two relays increases up to 100%, the current through backup relay reduces down to $I_{\mathrm{OCR1}}^{\min}$. In this condition, the thermal limit time of the network conductor for $I_{\mathrm{OCR1}}^{\max}$ is t_{mc}. In other words, if the network current is $I_{\mathrm{OCR1}}^{\max}$, the fault clearing time should be smaller than t_{mc}. But, since the current through the OCR1 is $I_{\mathrm{OCR1}}^{\min}$, it operates at t'_{OCR1} which is larger than the thermal limit of the network conductor. Usually, the maximum allowable operating time of the backup relay in the distribution systems is considered equal to 1000 ms. In other words, the characteristic curves of the main and backup protections should be located below the thermal limit curve. For this purpose, as shown in Fig. 2, by considering the maximum penetration level as the worst case of presence of PV systems and reducing I_{OCR1} related to this penetration level to $I_{\mathrm{OCR1}}^{\min}$, the operating time of OCR1 relay t'_{OCR1} should be reduced to t_{mc} below the I^2t curve. By doing this, the operating point of the backup relay which was changed due to the presence of PV systems is modified.

3.2 Presence of PV Sources Upstream from the Main and Backup Relays

If the PV sources are located upstream from the main and backup relays, the currents through the both relays increase depending on the penetration level of PV sources as

$$I_{\mathrm{OCR1}} = I_{\mathrm{OCR2}} = \frac{1}{Z_T}\left[V_S + \sum_{m=1}^{n} I_{\mathrm{PV}_m}\left(Z_F + \sum_{i=1}^{m} Z_i\right)\right]. \tag{8}$$

Since the currents through the main and backup relays increase, their operating times and time interval between two relays operation reduce. If the reduction of time interval between the operation of two relays is greater than the allowable limit, the operating point of the backup relay for the fault current $I_{\mathrm{OCR1}}^{\max}$ should be modified for restoring the protection coordination. To do this, the operating time of the backup relay for $I_{\mathrm{OCR1}}^{\max}$ should be increased with an allowable distance to I^2t curve in such a way that the time interval between the characteristic curves of the main and backup protections equals to the allowable limit. Thus, for the maximum penetration level of PV sources located at the upstream network, the operating time of the backup relay $t_{\min}$ is considered greater than that of the main relay which this increment is equal to the initial time interval $(t_{\min} = t'_{\mathrm{OCR2}} + \mathrm{CTI})$.

3.3 Presence of PV Sources Between and Upstream from the Main and Backup Relays Simultaneously

The PV sources may be simultaneously located between and upstream from the relays. If PV1 is the source at the upstream of backup relay and PV2 is located between main and backup relays, the current through the backup relay is calculated as

$$I_{\mathrm{OCR1}} = I_S + \left(\frac{Z_1 + Z_F}{Z_T}\right) I_{\mathrm{PV1}} - \left(\frac{Z_2 + Z_F}{Z_T}\right) I_{\mathrm{PV2}}. \tag{9}$$

Depending on the location of PV sources along the feeder, the backup relay current is greater or less than its initial value I_S. If the capacity of PV1 and PV2 is same $(I_{\mathrm{PV1}} = I_{\mathrm{PV2}} = I_{\mathrm{PV}})$, (9) is expressed as

$$I_{\mathrm{OCR1}} = I_S + \left(\frac{Z_1 - Z_2}{Z_T}\right) I_{\mathrm{PV}}. \quad (10)$$

Equation (10) shows that in the case of PVs located between and upstream from the relays, the effect of PV sources on the OCR1 is less than the case of PVs located between or upstream of the relays. Moreover, if the PVs distances to the backup relay are same $(Z_1 = Z_2)$, the PV sources do not affect the OCR1 current. In this condition, the current through the backup relay is equal to the current of upstream network $(I_{\mathrm{OCR1}} = I_S)$ which is similar to the case of no PV source in the network. Thus, in this paper, only the effects of PVs located between relays and PVs located upstream from the backup relay on the protection system are studied.

4 Proposed Scheme for Restoring the Protection Coordination

Since the presence of PV systems may disrupt the protection coordination of the distribution network, a comprehensive approach is required to analyze and reduce their effects on the system. Fig. 3 shows the proposed procedure for this purpose. In the first step, load flow is performed for initial settings of the protection system, determination of current transformer ratio, and measurement of load current. Then, the study starts for the case of occurring a fault in the network without any PV source. By executing the short circuit calculation, the branch currents are determined. In the next step, the operating times of the relays are determined based on their currents. Then, the operation of the protection system is evaluated. If the protection system is coordinate, the number of PV sources is increased which is proportional to increasing the penetration level of PV systems (maximum up to 100%). Since the protection coordination is lost in a specified penetration level of PV sources, the coordination is restored in the "coordination restoration using proposed method" section of the flowchart. Depending on the accessibility of protection device settings or PV control parameters, this section is implemented using two proposed strategies: (1) modified characteristic curve (MCC) strategy and (2) output current limiting (OCL) strategy. These strategies will be described in Subsections 4.1 and 4.2, respectively. It should be remembered that the calculations of the proposed coordination restoration method is performed offline. In other words, before the network operation, the proposed method should be executed for various locations of PV sources in the network and then, the modified settings are calculated.

4.1 Modified Characteristic Curve Strategy

Fig. 4(a) shows the new operating points of the backup protection for two scenarios of 100% penetration level of PV systems between and upstream of the relays, $\left[I^{\min}_{\mathrm{OCR1}}, t_{\mathrm{mc}}\right]$ and $[I^{\max}_{\mathrm{OCR1}}, t_{\min}]$, respectively, as the points P1 and P2. Based on the specified region between $t_{\min}$ and t_{mc}, the characteristic curve of the backup relay can be modified to satisfy the protection coordination. If the characteristic curve of the backup relay is implemented based on these points, the protection system is modified in such a way that the protection coordination is preserved between the main and backup relays and also between the backup relay and I^2t curve for all penetration levels and various locations of PV sources.

To regulate the operating curve of the backup relay, the parameters of the characteristic equation of the relay should be determined. In accordance with the standard IEC 60255 [34], this equation is defined as

$$t_{\mathrm{OCR1}} = \frac{A}{M^P - 1}\mathrm{TMS}, \quad (11)$$

where t_{OCR1} is the tripping time of the backup relay, TMS is the time multiplier setting, and M is the plug setting multiplier (PSM) and is defined as ratio of relay current to its plug setting current $I_{\mathrm{OCR1}}/I_{\mathrm{base}}$. A and P are constant parameters and they determine the slope of the protection characteristic curve. Since the proposed method aims to restore the protection coordination for all

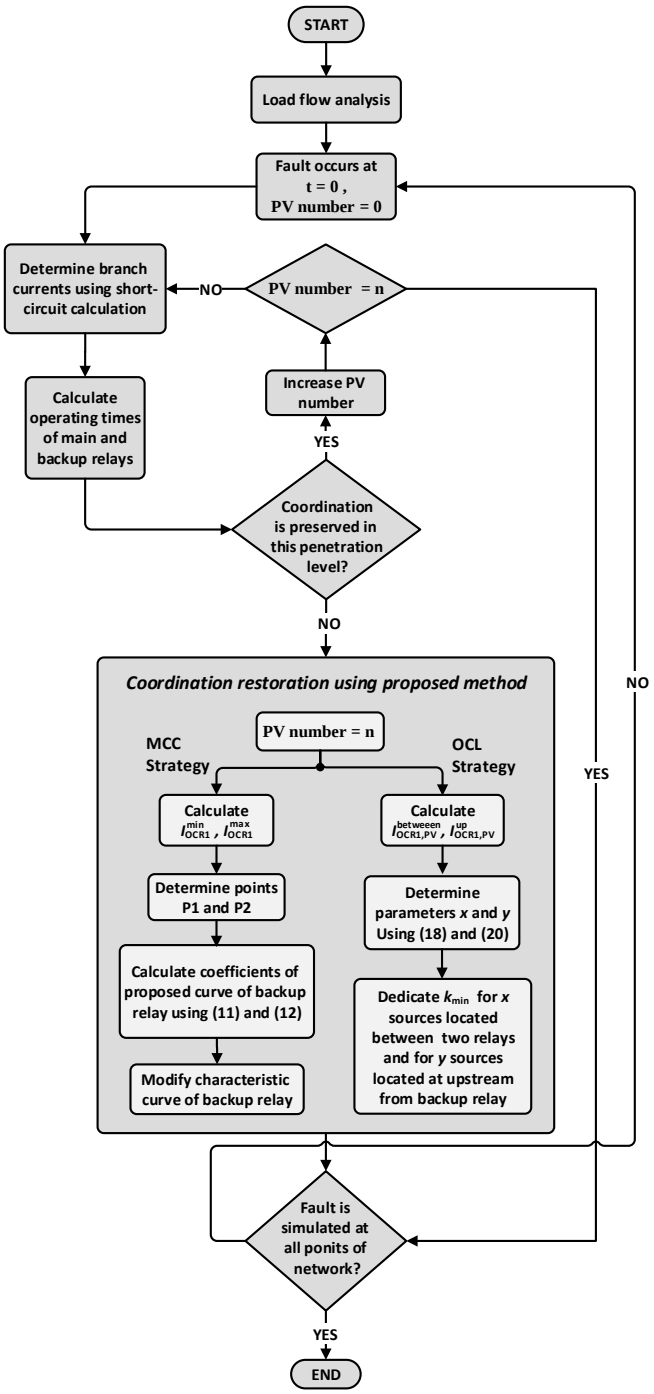

Fig. 3: Flowchart of the proposed procedure for investigating the effect of PV source presence on the network protection system.

PV arrangements by modifying the protection characteristic once, I_{base} and TMS is considered constant and the new characteristic is regulated using parameters A and P only.

By considering the presence of maximum penetration level of PV sources between and upstream from OCR1 and OCR2, the points P1 and P2 of the modified characteristic curve of the backup protection are determined. Using these points and (11), parameters A and P are calculated by solving (12) and (13) as

$$t_{\min} \times \left(M|_{I^{\max}_{\mathrm{OCR1}}}\right)^P - t_{mc} \times \left(M|_{I^{\min}_{\mathrm{OCR1}}}\right)^P + (t_{\mathrm{mc}} - t_{\min}) = 0, \quad (12)$$

$$A = \frac{t_{\min}}{\mathrm{TMS}}\left[\left(M|_{I^{\max}_{\mathrm{OCR1}}}\right)^P - 1\right]. \quad (13)$$

By regulating the characteristic curve of the backup protection OCR1 using A and P once, the protection system coordinately operates for all penetration levels of PV sources. The "coordination restoration using proposed method" section of Fig. 3 shows the flowchart of MCC strategy.

4.2 Output Current Limiting Strategy

Since the thermal inertia of the PV inverter is low, its current should be limited during the fault condition to protect the semiconductor switches [35]. The limited current is calculated as

$$I_{\mathrm{PV,SC}} = k \times I_{\mathrm{PV,n}}, \tag{14}$$

where $I_{\mathrm{PV,SC}}$ is the PV output current during a fault, $I_{\mathrm{PV,n}}$ is the nominal current of PV inverter, and k is the current increment factor which is usually adopted equal to two. OCL strategy aims to restore the protection coordination by adjusting current increment factor. However, selection of this parameter may affect the normal operation of the network. If k is a small value, the output current of PV is limited even for no fault events such as load increase. In regards of the impact of PV location on the current through the backup relay, the effect of PV source on the protection system can be controlled. Depending on the impact on the protection coordination, the proposed method limits k value only for those PV sources that further affect the protection coordination.

As shown in (4), the impact of PV sources on the current through the backup protection depends on their location. If the PV source is located between two relays and near the main one ($Z_1 \approx 0$), the current through the backup protection is very close to this current in the no PV case ($I_{\mathrm{OCR1}} \approx I_S$). If the PV source is near the backup relay ($Z_1 \approx Z_{\mathrm{Line2}}$), its effect on the OCR1 current is maximum ($I_{\mathrm{OCR1}} \approx I_S - I_{\mathrm{PV1}}$). Also, as stated in (8), if the PV source is located upstream from the backup protection and near this relay ($Z_1 \approx Z_{\mathrm{Line1}}$), the change of OCR1 current from its initial value is maximum ($I_{\mathrm{OCR1}} \approx I_S + I_{\mathrm{PV1}}$). However, if the distance of the PV source to the backup relay is high and PV is near the upstream network ($Z_1 \approx 0$), the backup protection current is less affected by the PV ($I_{\mathrm{OCR1}} \approx I_S$).

Equation (6) shows that the current through the backup protection is formed of two constant and variable terms. The former term I_S is affected by the upstream network while the latter one $I_{\mathrm{OCR1,PV}}$ depends on the penetration level of PV sources in the network and is expressed as

$$I_{\mathrm{OCR1,PV}} = \frac{1}{Z_T} \sum_{m=1}^{n} \left[I_{PV_m} \left(Z_F + \sum_{i=1}^{m} Z_i \right) \right]. \tag{15}$$

Thus, the backup relay current is $I_{\mathrm{OCR1}} = I_S - I_{\mathrm{OCR1,PV}}$. By controlling $I_{\mathrm{OCR1,PV}}$, the backup relay current which is deviated from its initial value can be preserved in the allowable range. Indeed, changing I_{OCR1}in its allowable limit preserves the backup protection coordination. As shown in Fig. 4(b), based on the specified time range for the backup relay $[t_{\min}, t_{\mathrm{mc}}]$, a current limit for this relay to preserve the protection coordination can be determined by controlling the PV currents. For this purpose, the maximum penetration level of the PV sources is considered. Depending on the location of PV systems (between two relays or upstream from the backup relay), different methods should be adopted.

4.2.1 Presence of PV Sources between Two Protection Relays: If in the worst case, i.e., the penetration level of 100%, the operating time of OCR1 is below the I^2t curve, the protection coordination is preserved for all penetration levels. Thus, the operating time of the backup relay for maximum penetration level of PV sources is considered equal to t_{mc}. Based on (9), the current through the backup relay is expressed as

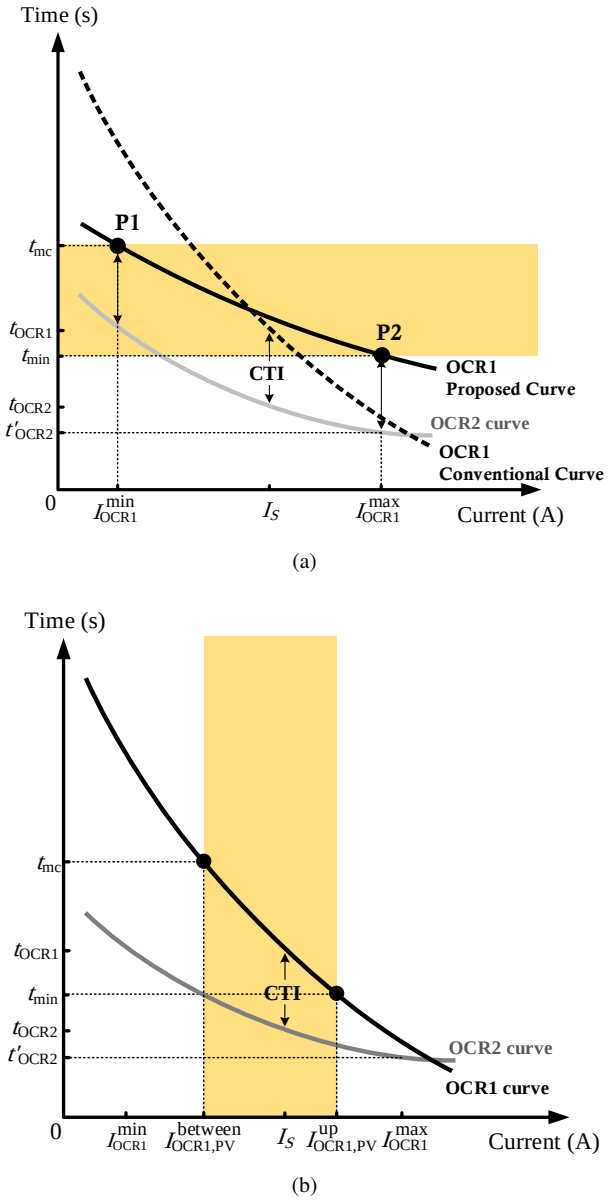

Fig. 4: Restoration of protection coordination using proposed scheme.
a Determination of modified characteristic curve of backup relay.
b Determination of allowable limit for injected current of PVs.

$$I_{\mathrm{OCR1}} = M|_{t_{\mathrm{OCR1}}=t_{\mathrm{mc}}} \times I_{\mathrm{base}} = \sqrt[P]{1 + \frac{A \times \mathrm{TMS}}{t_{\mathrm{mc}}}} \times I_{\mathrm{base}}. \tag{16}$$

The new backup relay current is calculated using (16) for which the protection coordination is preserved. Thus, that term of backup relay current which is affected by the penetration level of PV sources is determined as follows which is less than its previous value.

$$I^{\mathrm{between}}_{\mathrm{OCR1,PV}} = I_S - I_{\mathrm{OCR1}}. \tag{17}$$

This current reduction is implemented based on the PV location and its impact on the current through the backup relay. The locations of PVs are divided into two sections: less impact and more impact on the protection system. Those installed PVs which less deviate I_{OCR1} allow to deliver their maximum allowable fault current ($k_{\max} = 2$). However, the current increment factor of those PVs that further affect the current through the backup relay is reduced to the minimum value of current increment factor $k_{\min}$.

Using (15), the currents of these two sections are expressed as

$$I_{\mathrm{OCR1,PV}}^{\mathrm{between}} = I_{\mathrm{OCR1,PV}}^{\mathrm{between,more}} + I_{\mathrm{OCR1,PV}}^{\mathrm{between,less}} = \frac{1}{Z_T}\sum_{m=1}^{x}\left[k_{\min}\times I_n\left(\sum_{i=1}^{m} Z_i + Z_F\right)\right] + \frac{1}{Z_T}\sum_{m=x+1}^{n}\left[k_{\max}\times I_n\left(\sum_{i=1}^{m} Z_i + Z_F\right)\right], \quad (18)$$

where x is the number of those PV sources which their currents should be more limited based on the proposed method. Using (17), the parameter x is calculated by solving (18). Finally, the current increment factor of PV sources in that section is set to $k_{\min}$.

4.2.2 Presence of PV Sources at Upstream from Backup Protection: OCR2 current is calculated using (8) for the highest penetration level of PV sources. The operating time of the backup relay is equal to $t_{\min}$ and consequently, the backup relay current is calculated as

$$I_{\mathrm{OCR1}} = M|_{t_{\mathrm{OCR1}}=t_{\min}} \times I_{\mathrm{base}} = \sqrt[P]{1+\frac{A\times \mathrm{TMS}}{t_{\min}}}\times I_{\mathrm{base}}. \quad (19)$$

Using (19), the variable term of the backup relay current is calculated as

$$I_{\mathrm{OCR1,PV}}^{\mathrm{up}} = I_S - I_{\mathrm{OCR1}} = I_{\mathrm{OCR1,PV}}^{\mathrm{up,more}} + I_{\mathrm{OCR1,PV}}^{\mathrm{up,less}} = \frac{1}{Z_T}\sum_{m=1}^{y}\left[k_{\min}\times I_n\left(\sum_{i=1}^{m} Z_i + Z_F\right)\right] + \frac{1}{Z_T}\sum_{m=y+1}^{n}\left[k_{\max}\times I_n\left(\sum_{i=1}^{m} Z_i + Z_F\right)\right], \quad (20)$$

where y is the number of those PV sources installed at upstream feeder that further affect I_{OCR1}. By calculating y, the current increment factor of those PVs is set to $k_{\min}$.

The flowchart of the proposed method for restoring the protection coordination by controlling the inverter output current is shown in the "coordination restoration using proposed method" section of Fig. 3.

5 Simulation Results

In order to evaluate the effectiveness of the proposed coordination method, a section of the distribution system of the Isfahan city in the center of Iran is studied with the introduction of PV sources at various locations. Fig. 5 shows the single-line diagram of the study test system which is simulated in ETAP environment. This network consists of two 20 kV overhead three-wire system with radial configuration. The majority of loads are residential which are connected to the network using the 20 kV/400 V transformers. The parameters of the study system are presented in Table 1.

The OCR1 and OCR2 protect feeder 1 while feeder 2 is protected by OCR3. The protection zone of each protective device is shown in Fig. 5. In the normal operation, the feeders do not connect together. However, to continuous feeding of feeder 1 loads, there is an interlock between switches S and CB1. The switch S connects feeder 2 to feeder 1 when OCR1 is opened due to a no fault event. In this section, first, the coordinated operation of OCR1 and OCR2 is investigated in the cases of conventional and proposed strategies. Then, performance of the proposed scheme is evaluated when the feeder 2 is connected to the feeder 1 using switch S.

Table 1 Study Test System Parameters

Parameter	Specification
Length of feeder	30 km
Feeder type	Head way type & not transposed - radial
Conductor size	MV line = 120mm^2–LV line = cable 4×50+25mm^2
Line shape	Horizontal & distance between lines = 70,140,70cm
Nominal voltage	MV = 20 kV$_{LL}$, LV = 400 V$_{LL}$, 3ph+N+PE
Legs altitude	9 m
Transformer	630 kVA , Δ/y grounded, 20 kV / 0.4 kV
MVASC of main substation	500 MVA
PV inverter	200 kVA & tied grid without battery
Level of load unit	200 kVA

5.1 Performance Evaluation of Conventional Protection System

In accordance with conventional protection system of distribution networks, the feeders are protected using overcurrent relays as the main and backup protections while the fuses protect the laterals. The minimum coordination time interval between two protection devices is 350 ms for no disruption in their operations while the maximum value of this time is 1000 ms for no interference with the thermal limit curve.

When there is no PV source in the study system, the fault current at protection zone of OCR2 is maximum when a three-phase fault occurs at point F in the network side (20 kV) and it is 728 A. Based on the initial settings of protection system, the operating time of OCR2 for this current is 250 ms. If OCR2 fails, OCR1 operates after coordination time interval of 350 ms at $t = 600$ ms.

In the presence of PV sources in the network, they contribute the fault current depending on their penetration levels and locations. First, the penetration level of PV sources is assumed to be 10%. In this condition, if the PV sources are located between OCR1 and OCR2, the fault currents through the OCR1 and OCR2 are 863 A and 697 A, respectively, during a three-phase fault at point F. Thus, the operating times of the main and backup relays are 200 ms and 681 ms, respectively.

If PV sources are located upstream from backup protection and a fault occurs at point F, the currents through OCR1 and OCR2 are same and they change equally. In this case, the current of main and backup relays is 799 A. Based on the protection zones and fault location, the operating times of main and backup relays are 220 ms and 472 ms, respectively.

In comparison with no PV scenario, coordination time interval between OCR1 and OCR2 increases when PV sources are located between two relays. Consequently, the penetration level of 10% improves the protection system performance by increasing the operating time of the backup relay. Also, when the PV sources are located upstream of backup protection, the operating times of both relays reduce for penetration level of 10% and thus, the operation speed of protection system in clearing the fault increases.

Table 2 Performance of conventional and proposed protection systems in the presence of PV sources located between main and backup relays

PV Penetration Level	Conventional Strategy			MCC Strategy	OCL Strategy
	t_{OCR1}	t_{OCR2}	Δt	t_{OCR1}	t_{OCR1}
0	600	250	350	630	600
10	681	200	481	652	603
20	777	171	606	674	605
30	887	151	736	696	607
40	1014	137	877	717	609
50	1158	126	1032	738	629
60	1295	117	1178	756	677
70	1420	110	1310	772	720
80	1560	103	1457	783	750
90	1690	97	1593	791	780
100	1810	91.4	1718.6	797	799

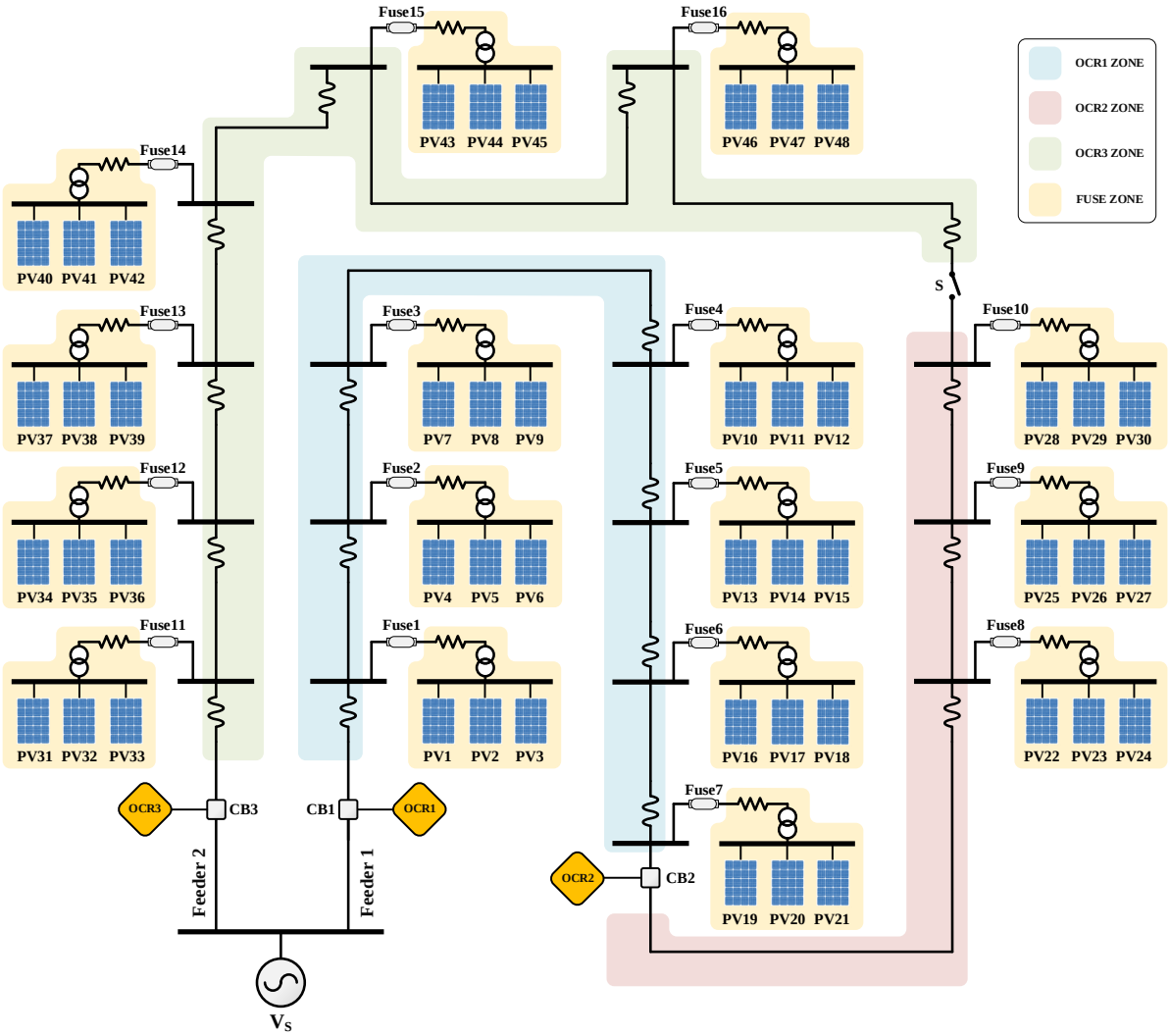

Fig. 5: Single-line diagram of the study test system.

When the PV sources are located between the main and backup relays and their penetration levels increase, the operating time of the backup relay increases. The impact of PV sources on the operating times of OCR1 and OCR2 in the conventional protection system is presented in Table 2. If the penetration level of PV sources is greater than 50%, the operating time of backup relay is greater than the thermal limit of 1000 ms. In the case of penetration level of 100%, the operating time of backup relay increases to 1810 ms. Fig. 6(a) shows the simulation result of main and backup relays when the conventional protection system is implemented in the study system. This figure shows the impact of PV sources on the protection characteristic curves when these sources are located between OCR1 and OCR2.

For penetration levels greater than 10%, the reduction of operating times of these relays limits the coordination time interval between them more. Table 3 shows the impact of PV sources located upstream from the main and backup relays on their operating times. If the penetration level of PV sources is 20%, the coordination time interval is less than the minimum limit of 250 ms. Fig. 6(b) shows the performance of conventional protection system when PV sources are located at upstream network. For the penetration level of 100%, coordination time interval reduces to 193 ms.

5.2 Performance Evaluation of Proposed Coordination Scheme

In the case of PV sources located between protection relays, the current through the backup relay is calculated using (6) for maximum penetration level of PV sources. Using this current, the operating time of backup relay t'_{OCR1} is determined using (11). To ensure proper performance of backup relay, the time interval of 200 ms is considered between the operating times of OCR1 and I^2t curve. Thus, the operating time of OCR1 for the maximum penetration level of 100% is allowable time of 800 ms. Indeed for the current of 557 A, the backup relay operates after 800 ms instead of operating time of 1810 ms in the conventional protection system.

When the PV sources are located upstream from both relays and MCC strategy is employed, the operating time of the backup protection is determined using (8) considering the operating time of OCR2 in penetration level of 100%. To do this, by considering the allowable initial time interval CTI from the operating time of OCR2, the trip command time of OCR1 is determined. In this condition, the operating time of the backup relay changes from 193 ms to 350 ms. If OCL strategy is used, OCR1 operating time $t_{\min}$ is set to 300 ms for the penetration level of 100%. In the next step, the parameters x and y are calculated using the proposed strategy.

By implementing the OCR1 characteristic curve matched on $t_{\min}$ and t_{mc} points, the protection coordination is preserved between OCR1 and OCR2 and also between OCR1 and I^2t curve for all penetration levels and locations of PV sources. If there is no PV source in the network, the coordination of protection system is also preserved.

Table 3 Performance of conventional and proposed protection systems in the presence of PV sources located upstream from backup relay

PV Penetration Level	Conventional Strategy			MCC Strategy	OCL Strategy
	t_{OCR1}	t_{OCR2}	Δt	t_{OCR1}	t_{OCR1}
0	600	250	350	630	600
10	472	220	252	588	595
20	419	206	213	567	588
30	395	200	195	556	584
40	383	197	186	551	555
50	378	195	183	549	543
60	376	195	181	547	538
70	375	194	181	546	536
80	374	194	180	545	535
90	373	194	179	544	535
100	372	193	179	543	535

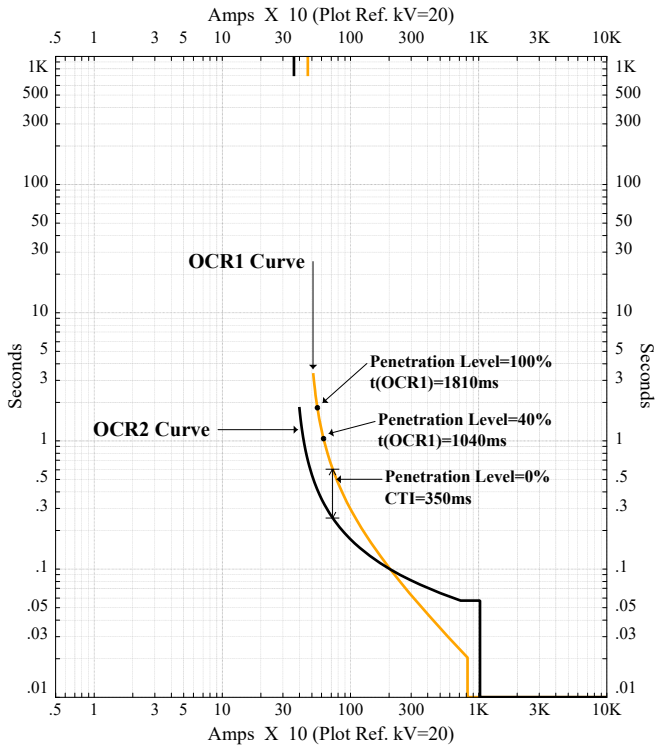

(a)

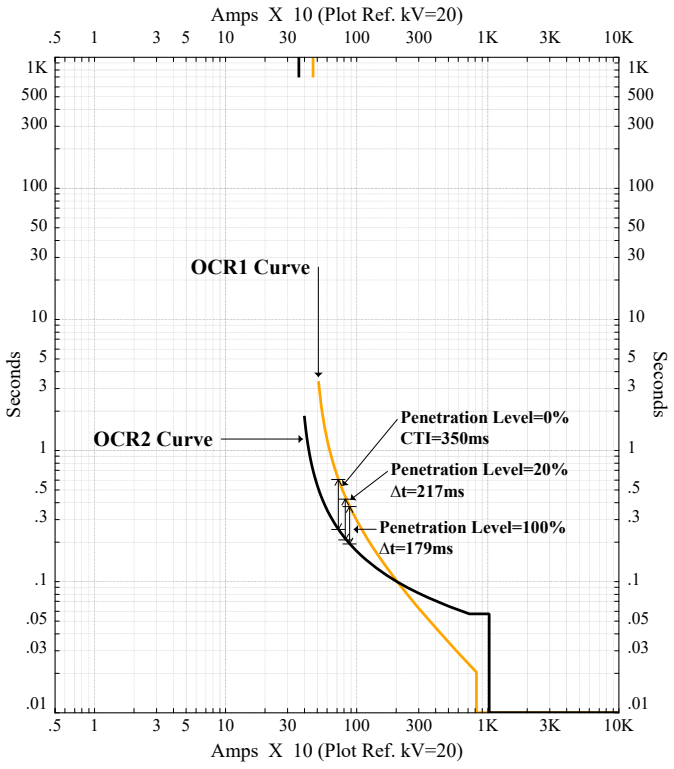

(b)

Fig. 6: Performance evaluation of the conventional protection system.
a PV sources located between two protection relays.
b PV sources located upstream from backup relay.

5.2.1 MCC Strategy: By modifying the characteristic curve of the backup relay, the MCC strategy preserves the limits of operating time of backup relay inside the coordination interval which is

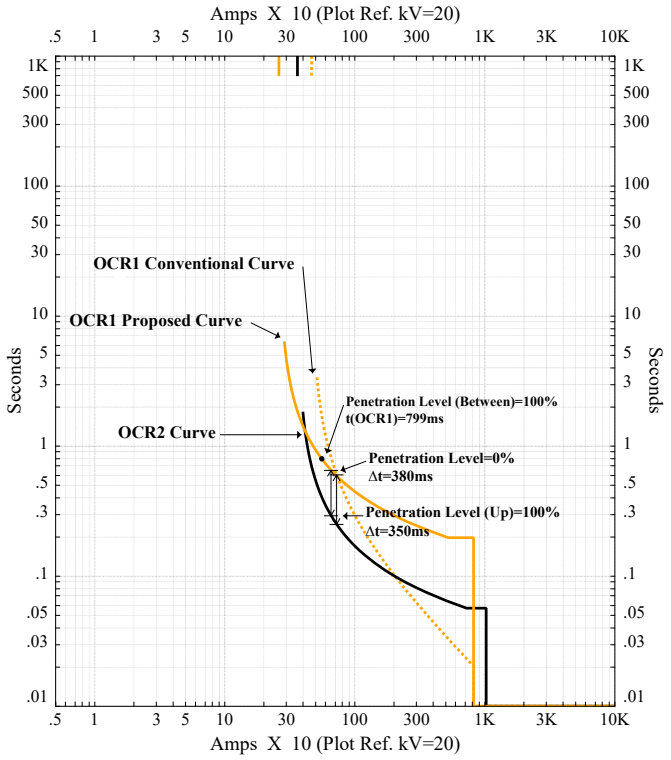

Fig. 7: Performance of MCC strategy in the presence of PV sources between and upstream from the relays.

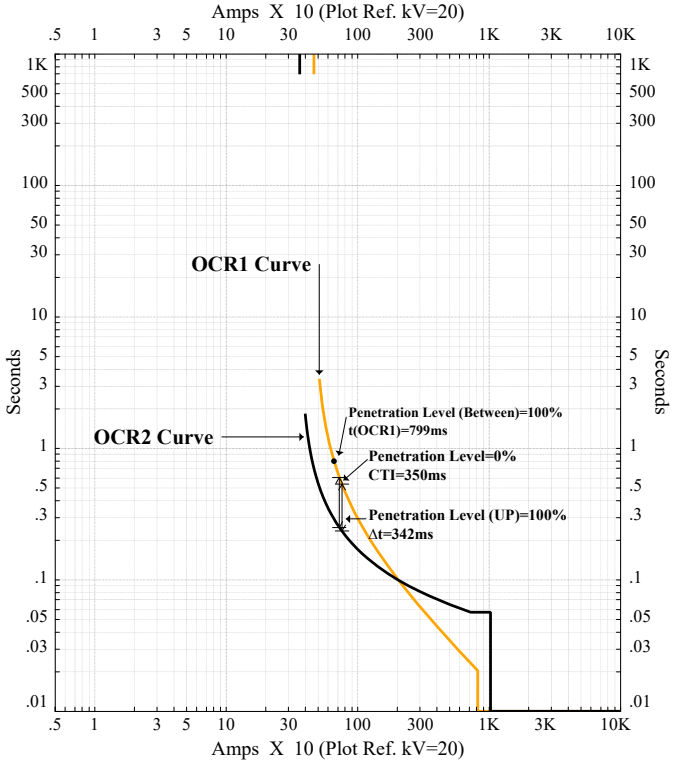

Fig. 8: Performance of OCL strategy in the presence of PV sources between and upstream from the relays.

specified by points P1 and P2. After determining these points, the new coefficients of backup relay characteristic curve are calculated using (12) and (13). Since the commercial relays are designed based on the standard, their characteristic curves are limited. Thus, to set the new characteristic on the relay, the nearest curve coefficients to the new coefficients are adopted. Thus in accordance with IEC standard, the proposed characteristic curve is a standard inverse curve. Table 2 presents the performance evaluation of backup relay when MCC strategy is used. By comparison with the conventional protection system, proper performance of the proposed method is observed for all penetration levels of PV sources. This proper operation is verified in Fig. 7 which shows the protection characteristic curves of the study system. Using new settings of OCR1, the time interval of 350 ms from OCR2 operating time is preserved for penetration level of 100%. In the case of presence of PV sources between the protection relays, the operating time of backup relay OCR1 is less than the thermal limit of the network conductor, as shown in Table 2.

5.2.2 OCL Strategy: OCL strategy adjusts the current increment factor of PV sources based on their impact on the protection system. Based on (18), the current increment factor of x sources which are located between two relays and near the backup protection is set to $k_{\min}$ while this factor for other sources is kept in the normal value of $k_{\max} = 2$. If the PV sources are installed at upstream from OCR1, based on (20), the current increment factor of y sources which are near the backup protection is set to $k_{\min}$ and this factor for other sources does not change ($k_{\max} = 2$). For the study system, the calculated x and y are 4 and 3, respectively, and $k_{\min}$ is considered equal to 1.3.

The performance of the proposed method in the cases of PV sources located between and upstream from the relays are shown in Tables 2 and 3, respectively. By using the new settings, the coordination between OCR1 and OCR2 is properly preserved for all penetration levels of PV sources. Fig. 8 shows the performance of OCL strategy which verifies that the current through the protection relays remains at allowable limits for all penetration levels and locations of PV sources.

As mentioned in Section 2, when there is no PV source in the network, OCR1 and OCR2 correctly operate in the current range $\left[I_F^{\min}, I_F^{\max}\right]$. M values for the minimum and maximum fault currents are 1.3326 and 1.8047, respectively. In the case of using conventional protection system, if the penetration level of the PV sources between and upstream from two relays increases up to 100%, M values are 1.1953 and 1.9013, respectively. These values are out of coordination range [1.3326 1.8047]. Since the MCC strategy does not affect the fault current, M values are same as the case of using conventional scheme. However, MCC strategy restores the protection coordination by modifying the operating time of the backup relay. When the OCL strategy is employed, M values for the cases of PV sources located between and upstream from the main and backup relays are 1.4227 and 1.6245, respectively, which are inside the coordination range [1.3326 1.8047]. Thus, the proposed strategy preserves the protection coordination even for the penetration level of 100%.

5.2.3 High-Impedance Fault: A high-impedance fault (HIF) occurs when an overhead conductor comes in contact with a high-impedance object such as the tree limbs, or breaks and falls on a high-impedance surface such as the asphalt road [36]. Since the fault resistance of an HIF is high, the current through the relays are relatively low during the fault condition. Table 4 shows the performance of the conventional and proposed protection schemes during a single-phase to ground HIF when the PV sources are located between the main and backup relays. When the conventional protection system is used, the protection coordination is lost in the penetration levels of 30% and 20% for the cases of fault resistance of 15 Ω and 30 Ω, respectively. However, both proposed strategies give satisfactory results for all penetration levels of PV sources. Although the operating time of relays increases due to relay current reduction, the proposed protection scheme preserves the coordination between the main and backup relays.

5.2.4 Network Topology Change: When the switch S is closed and the CB1 is opened, the feeder 2 connects to feeder 1. In this condition, OCR2 operates as the main relay while OCR3 operates

Table 4 Performance of conventional and proposed protection systems in the presence of PV sources located between main and backup relays in the case of high-impedance faults

PV Penetration Level	Conventional Strategy			MCC Strategy	OCL Strategy
	t_{OCR1}	t_{OCR2}	Δt	t_{OCR1}	t_{OCR1}
Fault resistance of 15 Ω					
0	609	259	350	627	609
10	711	243	468	644	625
20	839	232	607	662	642
30	1002	223	779	681	660
40	1208	216	992	701	679
50	1476	210	1266	722	702
60	1834	206	1628	744	728
70	2335	201	2134	767	757
80	3078	198	2880	791	788
90	3826	194	3632	816	820
100	4611	191	4420	842	853
Fault resistance of 30 Ω					
0	619	269	350	633	619
10	826	257	569	670	628
20	1076	247	829	704	638
30	1371	241	1130	736	648
40	1715	235	1480	765	658
50	2115	231	1884	791	692
60	2586	228	2358	816	729
70	3145	225	2920	839	767
80	3819	222	3597	860	808
90	4641	220	4421	880	851
100	5657	217	5440	899	897

Table 5 Performance of conventional and proposed protection systems in the presence of PV sources located between and upstream from main and backup relays in the case of network topology change

PV Penetration Level	Conventional Strategy			MCC Strategy	OCL Strategy
	t_{OCR3}	t_{OCR2}	Δt	t_{OCR3}	t_{OCR3}
PVs Located Between Relays					
0	600	250	350	622	600
10	669	245	424	639	609
20	744	240	504	655	620
30	824	236	588	673	635
40	911	232	679	690	661
50	1005	229	776	707	683
60	1106	226	880	725	705
70	1215	224	991	743	727
80	1332	221	1111	762	750
90	1457	219	1238	780	774
100	1592	217	1375	799	798
PVs Located Upstream From Relays					
0	600	250	350	662	600
10	542	237	305	635	596
20	497	227	270	614	592
30	461	218	243	597	588
40	432	212	220	582	578
50	409	206	203	570	570
60	389	201	188	560	562
70	373	197	176	551	555
80	359	194	165	543	548
90	347	191	156	537	542
100	337	188	149	533	536

as its backup relay. In the case of no PV source in the network, the operating times of the main and backup relays are 250 ms and 600 ms, respectively, and coordination time interval of 350 ms is preserved. When the penetration level of PV sources located between relays increases up to 50%, OCR3 operates at 1005 ms that leads to miscoordination of relays. Also, the coordination of relays is lost in the penetration level of 30% when the PV sources are located upstream from the relays. Table 5 shows the impact of PV sources located between and upstream from the main and backup relays on their operating times in the cases of using conventional and proposed strategies. The results verify the effectiveness of the proposed strategies in restoring the coordination of the main and backup relays.

6 Conclusion

The motivation of this paper is to preserve the protection coordination of radial distribution systems in the presence of PV sources with any penetration level and various locations. The protection coordination is restored by modifying the protection characteristic curve or limiting the PV inverter current. The study of the Isfahan distribution system with high penetration of PV sources shows that MCC strategy preserves the protection coordination even for the highest penetration level of PV sources without changing the available protection system structure. Also, it can be used in the old overcurrent relays. By determining those PV sources which further affect the protection system and further limiting their output currents during the fault, the OCL strategy improves the protection system performance without decreasing the output power of other PV sources. The proposed strategies do not require communication links and their calculations are offline.

7 References

1. Yan, B., Luh, P.B., Warner, G., Zhang, P.. Operation and design optimization of microgrids with renewables. *IEEE Transactions on Automation Science and Engineering* 2017;14(2):573–585. doi:10.1109/TASE.2016.2645761.
2. Zhang, W., Xu, Y., Liu, W., Ferrese, F., Liu, L.. Fully distributed coordination of multiple dfigs in a microgrid for load sharing. *IEEE Transactions on Smart Grid* 2013;4(2):806–815. doi:10.1109/TSG.2012.2234149.
3. Sadeghian, M., Fani, B.. Advanced localized reactive power sharing in microgrids. *Electric Power Systems Research* 2017;151:136–148. doi: http://dx.doi.org/10.1016/j.epsr.2017.05.028.
4. Joshi, K.A., Pindoriya, N.M.. Case-specificity and its implications in distribution network analysis with increasing penetration of photovoltaic generation. *CSEE Journal of Power and Energy Systems* 2017;3(1):101–113. doi: 10.17775/CSEEJPES.2017.0013.
5. Gomez, J.C., Vaschetti, J., Coyos, C., Ibarlucea, C.. Distributed generation: impact on protections and power quality. *IEEE Latin America Transactions* 2013;11(1):460–465. doi:10.1109/TLA.2013.6502846.
6. Doukas, D.I., Papastergiou, K., Bakas, P., Marinopoulos, A.. Energy storage sizing for large scale PV power plants base-load operation - comparative study & results. In: *38th IEEE Photovoltaic Specialists Conference*. 2012:000570–000574. doi:10.1109/PVSC.2012.6317678.
7. Hoke, A., Butler, R., Hambrick, J., Kroposki, B.. Steady-state analysis of maximum photovoltaic penetration levels on typical distribution feeders. *IEEE Transactions on Sustainable Energy* 2013;4(2):350–357. doi: 10.1109/TSTE.2012.2225115.
8. Camacho, A., Castilla, M., Miret, J., Vasquez, J.C., Alarcon-Gallo, E.. Flexible voltage support control for three-phase distributed generation inverters under grid fault. *IEEE Transactions on Industrial Electronics* 2013;60(4):1429–1441. doi: 10.1109/TIE.2012.2185016.
9. HernÃąndez, J.C., Vidal, P.G.. Guidelines for protection against electric shock in pv generators. *IEEE Transactions on Energy Conversion* 2009;24(1):274–282. doi:10.1109/TEC.2008.2008865.
10. Garcia, O., Hernandez, J.C., Jurado, F.. Guidelines for protection against overcurrent in photovoltaic generators. *Advances in Electrical and Computer Engineering* 2012;12(4):63–70. doi:10.4316/AECE.2012.04010.
11. HernÃąndez, J.C., Vidal, P.G., Jurado, F.. Lightning and surge protection in photovoltaic installations. *IEEE Transactions on Power Delivery* 2008;23(4):1961–1971. doi:10.1109/TPWRD.2008.917886.
12. Mozina, C.J.. Impact of smart grids and green power generation on distribution systems. *IEEE Transactions on Industry Applications* 2013;49(3):1079–1090. doi: 10.1109/TIA.2013.2253292.
13. HernÃąndez, J.C., De La Cruz, J., Vidal, P.G., Ogayar, B.. Conflicts in the distribution network protection in the presence of large photovoltaic plants: the case of endesa. *International Transactions on Electrical Energy Systems* 2013;23(5):669–688. doi:10.1002/etep.1623.
14. Saleh, K.A., Zeineldin, H.H., Al-Hinai, A., El-Saadany, E.F.. Optimal coordination of directional overcurrent relays using a new time–current–voltage characteristic. *IEEE Transactions on Power Delivery* 2015;30(2):537–544. doi: 10.1109/TPWRD.2014.2341666.
15. Rajaei, N., Ahmed, M.H., Salama, M.M.A., Varma, R.K.. Fault current management using inverter-based distributed generators in smart grids. *IEEE Transactions on Smart Grid* 2014;5(5):2183–2193. doi:10.1109/TSG.2014.2327167.

16. HernÃąndez, J., la Cruz, J.D., Ogayar, B.. Electrical protection for the grid-interconnection of photovoltaic-distributed generation. *Electric Power Systems Research* 2012;89(Supplement C):85 – 99. doi: https://doi.org/10.1016/j.epsr.2012.03.002.
17. Ebrahimpour, M., Vahidi, B., Hosseinian, S.H.. A hybrid superconducting fault current controller for DG networks and microgrids. *IEEE Transactions on Applied Superconductivity* 2013;23(5):5604306–5604306. doi: 10.1109/TASC.2013.2267776.
18. Varma, R.K., Rahman, S.A., Atodaria, V., Mohan, S., Vanderheide, T.. Technique for fast detection of short circuit current in PV distributed generator. *IEEE Power and Energy Technology Systems Journal* 2016;3(4):155–165. doi:10.1109/JPETS.2016.2592465.
19. Piesciorovsky, E.C., Schulz, N.N.. Fuse relay adaptive overcurrent protection scheme for microgrid with distributed generators. *IET Generation, Transmission Distribution* 2017;11(2):540–549. doi:10.1049/iet-gtd.2016.1144.
20. Sinclair, A., Finney, D., Martin, D., Sharma, P.. Distance protection in distribution systems: How it assists with integrating distributed resources. *IEEE Transactions on Industry Applications* 2014;50(3):2186–2196. doi: 10.1109/TIA.2013.2288426.
21. Chaitusaney, S., Yokoyama, A.. Prevention of reliability degradation from recloser–fuse miscoordination due to distributed generation. *IEEE Transactions on Power Delivery* 2008;23(4):2545–2554. doi:10.1109/TPWRD.2007.915899.
22. Hussain, B., Sharkh, S.M., Hussain, S., Abusara, M.A.. An adaptive relaying scheme for fuse saving in distribution networks with distributed generation. *IEEE Transactions on Power Delivery* 2013;28(2):669–677. doi: 10.1109/TPWRD.2012.2224675.
23. Dewadasa, M., Ghosh, A., Ledwich, G.. Fold back current control and admittance protection scheme for a distribution network containing distributed generators. *IET Generation, Transmission Distribution* 2010;4(8):952–962. doi: 10.1049/iet-gtd.2009.0614.
24. Wan, H., Li, K.K., Wong, K.P.. An adaptive multiagent approach to protection relay coordination with distributed generators in industrial power distribution system. *IEEE Transactions on Industry Applications* 2010;46(5):2118–2124. doi:10.1109/TIA.2010.2059492.
25. Sortomme, E., Venkata, S.S., Mitra, J.. Microgrid protection using communication-assisted digital relays. *IEEE Transactions on Power Delivery* 2010;25(4):2789–2796. doi:10.1109/TPWRD.2009.2035810.
26. Al-Sabounchi, A.M., Gow, J., Al-Akaidi, M.. Optimal sizing and location of large PV plants on radial distribution feeders for minimum line losses. In: *4th International Conference on Electric Power and Energy Conversion Systems (EPECS)*. 2015:1–7. doi:10.1109/EPECS.2015.7368528.
27. Khatod, D.K., Pant, V., Sharma, J.. Evolutionary programming based optimal placement of renewable distributed generators. *IEEE Transactions on Power Systems* 2013;28(2):683–695. doi:10.1109/TPWRS.2012.2211044.
28. Salem, M.M., Elkalashy, N.I., Atia, Y., Kawady, T.A.. Modified inverter control of distributed generation for enhanced relaying coordination in distribution networks. *IEEE Transactions on Power Delivery* 2017;32(1):78–87. doi:10.1109/TPWRD.2016.2555791.
29. Ahn, M.C., Ko, T.K.. Proof-of-concept of a smart fault current controller with a superconducting coil for the smart grid. *IEEE Transactions on Applied Superconductivity* 2011;21(3):2201–2204. doi:10.1109/TASC.2010.2091386.
30. Jo, H.C., Joo, S.K., Lee, K.. Optimal placement of superconducting fault current limiters (SFCLs) for protection of an electric power system with distributed generations (DGs). *IEEE Transactions on Applied Superconductivity* 2013;23(3):5600304–5600304. doi:10.1109/TASC.2012.2232958.
31. Hung, D.Q., Mithulananthan, N., Lee, K.Y.. Determining PV penetration for distribution systems with time-varying load models. *IEEE Transactions on Power Systems* 2014;29(6):3048–3057. doi:10.1109/TPWRS.2014.2314133.
32. Srivastava, A.K., Kumar, A.A., Schulz, N.N.. Impact of distributed generations with energy storage devices on the electric grid. *IEEE Systems Journal* 2012;6(1):110–117. doi:10.1109/JSYST.2011.2163013.
33. IEC standard for short-circuit currents in three-phase a.c. systems. *IEC Standard 60909* 2003;.
34. IEC standard for single input energizing quantity measuring relays with dependent or independent time. *IEC standard 60255* 2009;.
35. Sadeghkhani, I., Hamedani Golshan, M., Guerrero, J., Mehrizi-Sani, A.. A current limiting strategy to improve fault ride-through of inverter interfaced autonomous microgrids. *IEEE Transactions on Smart Grid* accepted for publication, Jan. 2016;doi:10.1109/TSG.2016.2517201.
36. Shah, P.H., Bhalja, B.R.. New adaptive digital relaying scheme to tackle recloser-fuse miscoordination during distributed generation interconnections. *IET Generation, Transmission Distribution* 2014;8(4):682–688. doi:10.1049/iet-gtd.2013.0222.